

Role of electronic excitation in phase-change memory materials: A brief review

X.-B. Li¹, X. Q. Liu², X. D. Han², and S. B. Zhang^{*1,3}

¹ State Key Laboratory on Integrated Optoelectronics, College of Electronic Science and Engineering, Jilin University, Changchun 130012, P.R. China

² Institute of Microstructure and Property of Advanced Materials, Beijing University of Technology, Beijing 100022, P.R. China

³ Department of Physics, Applied Physics, & Astronomy, Rensselaer Polytechnic Institute, Troy, New York 12180, USA

Received 15 June 2012, revised 3 August 2012, accepted 6 August 2012

Published online 24 September 2012

Dedicated to Stanford R. Ovshinsky on the occasion of his 90th birthday

Keywords athermal data storage, electronic excitation, Ge–Sb–Te, solid-state phase transition

* Corresponding author: e-mail zhangs9@rpi.edu, Phone: (518) 2766310, Fax: (518) 2766680

Phase-change memory (PCM) materials, such as chalcogenide alloys, have the ability for fast and reversible transition between their amorphous and crystalline states. Owing to the large optical/electrical contrast of the two states, PCM materials have been developed for data storage. It has been generally accepted that thermal effects, caused by laser irradiation or electrical pulses, control the amorphization by melting the sample and subsequent quenching, while crystallization is realized by thermal annealing. An important element that has not been considered extensively, however, is the role of electronic excitation by optical or

electrical pulse. Strictly speaking, until electrons and holes recombine, the system under external stimulus is in a non-equilibrium environment, especially when the excitation intensity is high. This raises an important question: can the excitation alone induce phase transition for PCM data storage without the usual thermal melting? Here, we will review the recent experimental and theoretical indications and evidence in support of the electronic excitation-induced phase change in PCM materials and discuss potential ramifications of the athermal phase-change phenomenon for data storage.

© 2012 WILEY-VCH Verlag GmbH & Co. KGaA, Weinheim

1 Background The seminal work [1] by Sir S. R. Ovshinsky, to whom this special volume has been dedicated to, laid the cornerstone for phase-change memory (PCM) materials. Since then, PCM has attracted considerable attention because of its technical importance in optical storage and nonvolatile electronic memory. Needless to say, many efforts have been made and are discussed in this volume. Here, we only refer to a few of them [2–5] that improve the storage speed, reversible cycle, or stability during device performance. The so-called device is actually a layer of PCM material, which can rapidly switch between its bi-stable states induced by a laser or electrical pulse. Usually, the two states are represented by two distinct structural phases: the low-reflectivity, high-resistivity amorphous phase and the high-reflectivity, low-resistivity crystalline phase. The comprehension of the transition processes between the two phases is essential to the understanding and exploration of high-performance PCM devices.

In current PCM devices, there is no doubt that thermal heating dominates [3], for which laser and electrical pulse

serve as an external heat source. In such a process, the PCM material starts as a crystal; once the temperature is raised to or above the liquidus point (T_m), the material melts; the resulting liquid is then rapidly quenched to room temperature to become amorphous. To get back to the crystalline state, the amorphous state is annealed at a temperature near the glass transition temperature (T_g), which is necessary for the nucleation and growth of the crystalline state. The current working speed of a PCM device is limited to a time scale of several nanoseconds for amorphization and several tens of nanoseconds for crystallization [3].

Increased switching speed is necessary if PCM devices are to compete more effectively with other storage techniques. The roads toward the goal, however, differ from each other in several ways: (i) by the optimization of the PCM alloys with different elemental compositions [6], (ii) by the design of new devices [7], and (iii) by the selection of external field pulse [8, 9]. No matter which method is employed, it is common practice to manipulate the phase

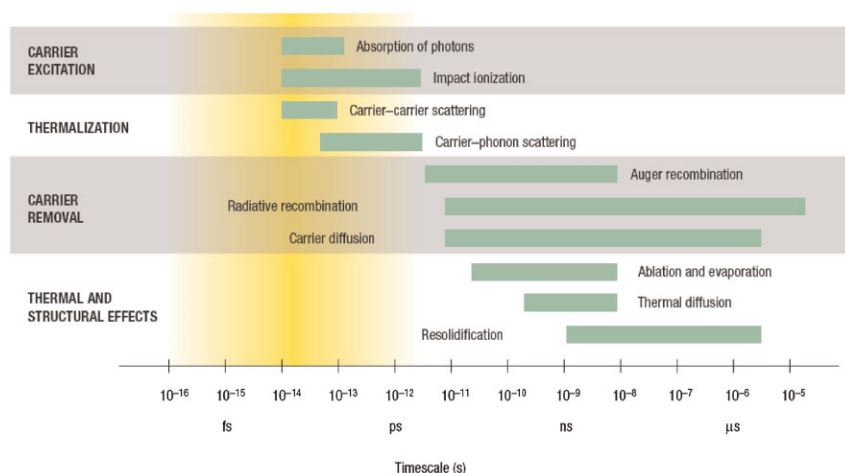


Figure 1 (online color at: www.pss-b.com) Time evolution of different electronic and lattice events for solid after femtosecond laser exposure. Figure reproduced with permission from Sundaram *et al.* [10]. © 2002 Nature Publishing Group.

transition with lesser atomic displacement while maintaining a large enough signal contrast.

To facilitate the discussion, let us consider the various processes in which a solid is exposed to an external pulse. One example is a laser pulse. It is generally accepted that a laser pulse with a duration of several nanoseconds or longer can replace a thermal source, as there is sufficient time for the photo-generated electron–hole (e–h) pairs to non-radiatively recombine. There exists, however, an initial period of electron-hole pair production by the excitation before any noticeable e–h recombination, either radiatively or non-radiatively, can take place. This period is typically much shorter in time, ranging from femtoseconds to 10 ps. Figure 1 [10] depicts a general picture for the interplay between electron and lattice dynamics by an fs laser-pulse excitation. It shows that the e–h recombination takes place in the time range of 10 ps to 10 ns after the initial excitation. Before the recombination, electrons and holes co-exist in the material as e–h plasma. Prior works have proposed a concept that the e–h plasma softens the lattice and induces phase transition at temperature well below T_m [11–13]. In the earlier experiments, Mazur [14] and von der Linde [15] observed a plasma-induced phase change in Si and GaAs to within 1 ps. This ultrafast transition is at least two orders of magnitude faster than the typical transitions for PCM materials. A faster forward phase change may also be correlated to a reverse phase change.

This raises an important question: can a plasma-induced phase transition take place in PCM materials and be used for even faster data storage? As early as 2004, Kolobov [4] argued that “*electronic excitation creating non-equilibrium charge carriers is crucial for the weakening and subsequent rupture of the subsystem of weaker Ge–Te bonds.*”

2 Early laser pump-probe ultrafast spectra on PCM materials Real time detection of phase transition in PCM materials is a key to the understanding of the salient physics. In the pump–probe experiment, one laser pulse is used to pump the material to create phase change, whereas another laser pulse is used to probe instantaneously the

reflected or transmitted signal during the phase-change process. The technique enables the identification of various stages experienced by the material during the transition and their time duration. In this regard, Siegel and co-workers have pioneered the study of the PCM mechanism by the pump-probe technique [8, 9, 16, 17]. It has been demonstrated by ns/sub-ns time resolution experiments that the amorphization of Ge–Sb–Te (GST) alloys undergoes through a liquid phase with optical properties different from either the crystalline or the amorphous state [18].

One can thus use the transient reflectivity technique to study melting during phase change. The first interesting work is perhaps the one in 2004 [8]. Figure 2 shows the real-time evolution of the reflectivity during the phase transition of GST induced by a 30-ps laser pulse. While it has been assumed that the reflectivity of liquid GST is in between those of crystalline and amorphous GST (see Fig. 2),

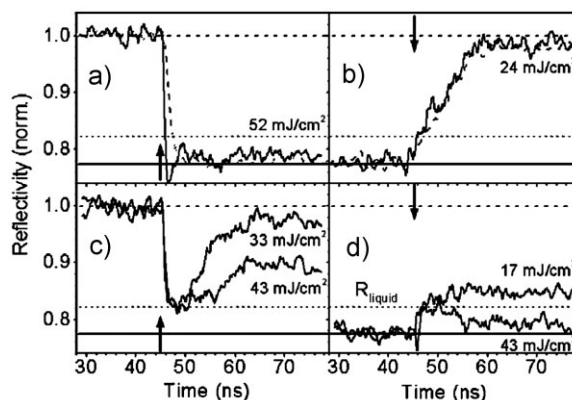


Figure 2 Reflectivity evolution during single ps laser pulse induced (a) amorphization and (b) crystallization in $\text{Ge}_2\text{Sb}_2\text{Te}_5$. (c) Amorphization attempts and (d) crystallization attempts with other laser fluence values in the same sample. The horizontal dashed line is for crystalline reflectivity, the horizontal solid one is for amorphous reflectivity. The horizontal dotted line is denoted as the liquid reflectivity in the original reference. Figure reproduced with permission from Siegel *et al.* [8]. © 2004 American Institute of Physics.

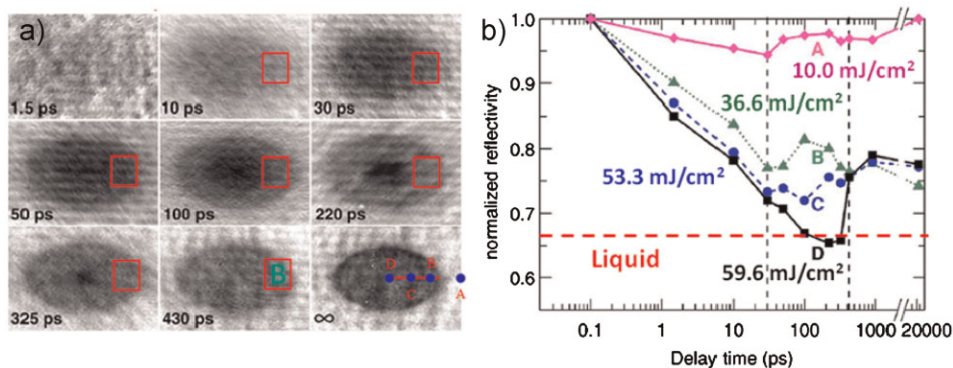


Figure 3 (online color at: www.pss-b.com) (a) Time-resolved surface reflectivity images of a crystalline $\text{Ge}_2\text{Sb}_2\text{Te}_5$ film at different delay times after exposure to a fs pump pulse. The frame size is $153 \times 101 \mu\text{m}$. (b) Temporal evolution of reflectivity (at 400 nm) at the characteristic radial position A, B, C, D from outside to the laser-focused center spot. Due to the Gaussian distribution of laser energy on focused area, the fluence from D to A drops from 59.6 to 10.0 mJ cm^{-2} . A special spot B (36.6 mJ cm^{-2}) is highlighted with red squares during the evolution in (a). The liquid reflectivity is also indicated as a dashed line based on our understanding of the physical process. Figure reproduced with permission from Siegel *et al.* [9]. © 2008 American Institute of Physics.

Ref. [18] suggested that the transient reflectivity of liquid GST should be lower than either crystalline or amorphous GST. According to this interpretation, Fig. 2(a) can be identified as a normal melt-quench amorphization process by a laser pulse of 52 mJ cm^{-2} because the reflectivity has gone through the lowest value before the system stabilizing in the amorphous state. The results at lower fluence of 33 or 43 mJ cm^{-2} in Fig. 2(c), however, need to be reinterpreted in contrast to the original explanation of slow cooling for the melt. Here, the reflectivity first drops down to that of an amorphous-like state and then rises back up toward that of a crystalline-like state, without going below that for liquid phase. Therefore, there is no melting taking place. As a matter of fact, if, at 33 and 43 mJ cm^{-2} , the samples indeed melt, they would be more easily amorphized, since lesser energy needs to be removed from the system to stabilize the amorphous state. However, that did not happen.

The second interesting work is the one in 2008 [9]. Here, amorphization of $\text{Ge}_2\text{Sb}_2\text{Te}_5$ was attempted with fs laser pulse. A pump ($\lambda = 800 \text{ nm}$) – probe ($\lambda = 400 \text{ nm}$) ultrafast spectrum traces the dynamics of amorphization by real-time reflectivity. The results are shown in Fig. 3. It is known that the local fluence in a laser pulse obeys Gaussian-type distribution, from which the fluence of the local spots in Fig. 3(b) has been evaluated. From the center point D along the horizontal line outwards to points C, B, A, they are 59.6, 53.3, 36.6, and 10 mJ cm^{-2} , respectively. Figure 3(a), on the other hand, shows the time evolution of the optical images. Their analysis suggested that the center spot D (59.6 mJ cm^{-2}) must experience a liquid state before getting to a steady amorphous state, which is supported by the especially low reflectivity during the 100–300 ps after the excitation. For comparison, we indicate in Fig. 3(b) the reflectivity of the liquid state. The low reflectivity is consistent with the dark images exhibited around the center spot at 100, 220, and 325 ps, respectively. What is more interesting in Fig. 3(a), however, is spot B with 36 mJ cm^{-2}

fluence (marked by us with red squares, and the original interpretation is also the melt followed by quenching), for which in fact there is no corresponding reflectivity in Fig. 3(b) that would indicate a liquid state. This is another example that phase transition may not go through the liquid state, but rather is a direct solid-to-solid process from crystalline state to amorphous state.

3 Theoretical study of amorphization under excitation for PCM

The analysis above prompts us to consider a possible athermal mechanism for PCM, which would be drastically different from the traditional thermal one. To pursue the matter further, we carried out a first-principles molecular dynamics (MD) study [19]. Note that using first-principle MD with optical excitation is currently a formidable task, as it requires the inclusion of electron-hole dynamics with a time step in attoseconds. Such calculations by time-dependent density functional theory (TDDFT) method [20] usually limit the simulation time to no more than 100 fs. In contrast, most of the dynamic processes involved in phase change have a time scale significantly larger than 1 ps. In our study, we have focused on the qualitative features rather than the quantitative results. Therefore, we simplify the study by removing electrons from the high-lying valence band states according to the strength of the excitation. In analogy to defect study, we used a jellium background charge to compensate for the loss of charged carriers.

As it turns out, it is useful to analyze the energy-dependent atomic distributions of the charge density for the crystalline state before phase change. Figure 4(a) shows for rock-salt (RS) GST the elemental- and orbital-dependent density of states (DOS) near the valence band maximum (VBM). As one might expect, Te *p* states dominate the DOS in this energy range. Besides the Te, we also notice the contributions from Ge and Sb *s* orbitals, in which the Ge contribution is noticeably larger than that of Sb.

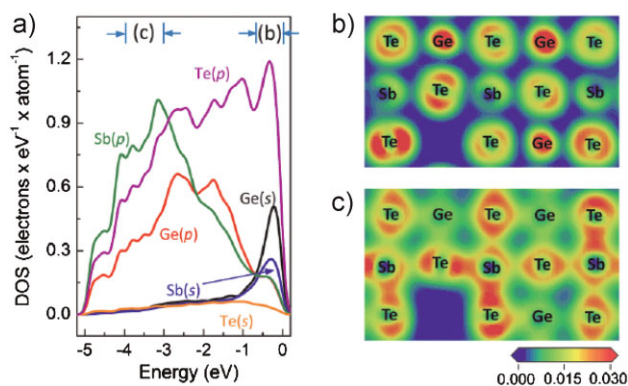


Figure 4 (online color at: www.pss-b.com) (a) Orbital-decomposed local DOS normalized by the number of corresponding element, Ge, Sb, and Te, respectively. (b) and (c) Charge density plots in the (100) plane in units of $e\text{\AA}^{-3}$: (b) is for states near the VBM from -0.66 to 0 eV and (c) is for states at deeper energies from -4 to -3 eV, as indicated by the letters (b) and (c) in panel (a). Figure reproduced from Li *et al.* [19]. © 2011 American Physical Society.

Figures 4(b and c) show the real-space charge distribution at two different energy windows: from -0.66 to 0 eV and from -4.0 to -3.0 eV, respectively. We see in Fig. 4(b) that the electrons reside primarily near Ge and its surrounding Te. In contrast, in Fig. 4(c) the electrons reside primarily near Sb and its surrounding Te. In other words, the absorption of the excitation is cation selective.

To see if the excitation can effectively lower the amorphization temperature (T_a), we carried out MD simulations at around or below T_m as low as 600 K. In the left panel of Fig. 5, we show several snapshots for the excitation induced amorphization along with the change of the coordination number (CN). In this particular run, a 15 ps excitation at 700 K (which is significantly smaller than T_m of about 1000 K [19]) is carried out and is followed by a 9 ps quench at 300 K. The crystal structure starts at RS [Fig. 5(a)]. After only 0.45 ps [Fig. 5(b)], the Ge coordination number, CN(Ge), is reduced from the original 6 to either 5 or 4 for every Ge, despite that on visual grounds the overall crystal structure remains largely intact. After 9 ps [Fig. 5(e)], the

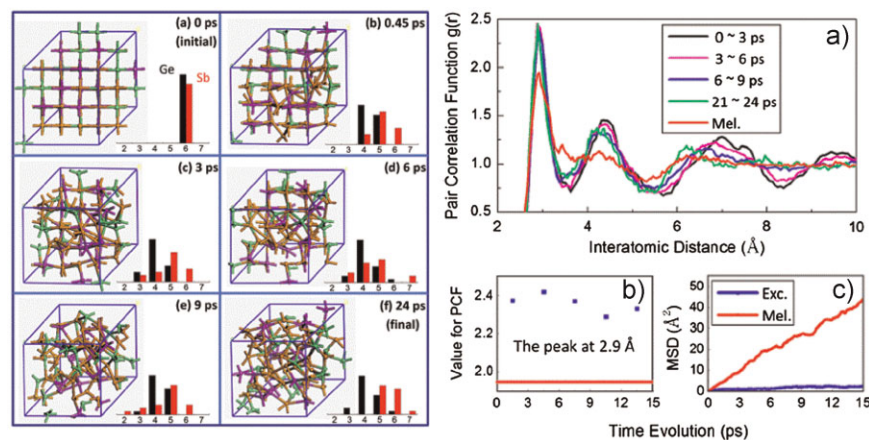


Figure 5 (online color at: www.pss-b.com) Dynamic evolution of amorphization under 9% electronic excitation for GST. Left panel shows the change of atomic structure and their coordination number. Right panel shows the evolution of PCF, PCF at 2.9 Å and MSD. Figure reproduced from Li *et al.* [19]. © 2011 American Physical Society.

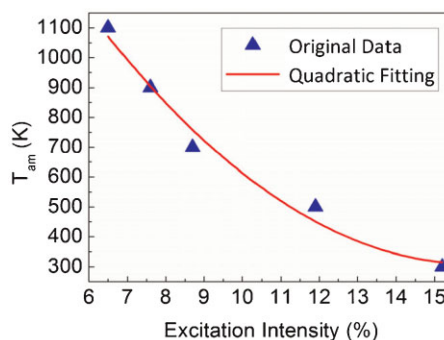


Figure 6 (online color at: www.pss-b.com) Calculated amorphization temperature T_a versus excitation intensity. Red line is a quadratic fitting to show the nonlinear dependence of T_a on the excitation.

GST becomes amorphous. Importantly, such an amorphization takes place without any melting. This indicates that phase change under excitation is indeed a solid to solid transition, which is expected to be considerably faster than amorphization via melting. Figure 5(f) shows that the amorphous structure remains after a 9 ps quench. The CNs are similar to those in Fig. 5(e), except for a significant population increase for CN(Sb) = 6. This is a consequence of placing back the removed electrons in the simulation, which is a necessary step to mimic the recombination of e-h pairs.

The right panel of Fig. 5 shows the pair correlation function (PCF) and mean square displacement (MSD) analyses for the run. They provide further evidence that the present GST amorphization process is in contrast to the normal melt-quench process. A significantly smaller MSD also suggests that the reverse process, namely, recrystallization, may be easier. Our explanation of the results is that with the removal of the Ge-dominated electrons (in the anti-bonding states) by excitation, Ge atoms will tend to form a tetrahedral coordination. This creates an instability that drives the amorphization of the GST at a significantly lower temperature than T_m . In principle, electrons in the conduction band can also weaken the bonds in GST. However, as it turns out, the effect of the holes in the valence band is considerably larger and, hence, more significant [19].

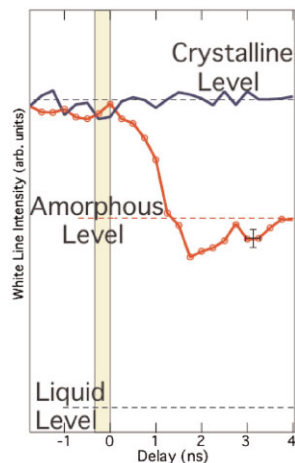


Figure 7 (online color at: www.pss-b.com) Evolution of white line intensity of the XANES during amorphization of $\text{Ge}_2\text{Sb}_2\text{Te}_5$ induced by a 600-ps duration laser pulse. Three dashed lines are shown for the corresponding static crystalline, amorphous, and liquid level, respectively. Figure reproduced with permission from Fons *et al.* [22]. © 2010 American Physical Society.

Figure 6 shows the calculated T_a as a function of the excitation intensity N_{e-h} . The simulations were done for T_a in the range from room temperature (300 K) to around experimental T_m . All simulations use the same procedure as described above: namely, a 15-ps excitation followed by a 9-ps annealing at 300 K in which the excited electrons have been placed back to mimic recombination. The results show clearly the tendency of decreasing T_a with increasing N_{e-h} [11]. A quadratic fitting shows that there is a nonlinear relationship between T_a and N_{e-h} at high excitations. Interestingly, the results show that for excitation $\geq 15\%$ phase transition can take place within 24 ps even at room temperature. Our analysis in Ref. [9] indicates that 17.6% excitation corresponds to $F = 36.6 \text{ mJ cm}^{-2}$.

4 Recent dynamic XANES observation during PCM amorphization X-ray absorption near-edge structure (XANES) is a powerful tool to monitor structure evolution. This happens because in the strong multiple-scattering regime, XANES provides a unique and robust “mapping” of three-dimensional structure around the X-ray-absorbing atom within a radius of a few nm [21]. Fons *et al.* [22] have employed an optical pump and XANES probe technique to detect the structural variation during $\text{Ge}_2\text{Sb}_2\text{Te}_5$ amorphization. Figure 7 shows a signal evolution of the white-line intensity from XANES after a 600-ps laser pump. If we focus on the red line, we see clearly that the crystalline level drops directly to the amorphous level within 1 ns and stabilizes at the level in 4 ns. Throughout the process, all the transient levels are considerably higher than the static liquid level. This experimental result therefore offers the solid proof that amorphization does not have to go through any melting. Fons *et al.* argued that the rupture of sacrificial (resonant) bonds under electronic excitation leads to the collapse of the ordered phase.

5 Comparison of the experimental conditions for laser-induced amorphization of PCM materials

Table 1 lists the experimental conditions for laser-induced amorphization, along with our MD simulation. It shows that *the amorphization behavior of the GST is strongly correlated with the laser pulse duration*. When a ns to sub-ns laser pulse is applied, the amorphization is clearly melting driven. But when a shorter pulse is applied, such as with pulse duration below tens ps to fs, the situation changes qualitatively. As one can see in Ref. [8], the transition induced by a 30-ps pulse (33 or 43 mJ cm^{-2}) did not go through the melting phase. Reference [9] suggests that with a fluence of 36.6 mJ cm^{-2} amorphization needs not go through the liquid phase either. Interestingly, at low pulse duration, amorphization without melting can be accomplished within 500 fs [23]. Overall, shorter duration leads to more significant athermal effects. This is because the transient

Table 1 Comparison of laser excitation conditions, which indicates that a melting of the crystal may not be the necessary condition for GST amorphization.

works	laser duration	laser fluence	amorphization time	melt?
optical probe [17]	4 ns	–	5 ns	yes
optical probe [9]	ns scale	154 mJ cm^{-2}	< 20 ns	yes
optical probe [18]	510 ps	$0.31 \text{ nJ pulse}^{-1}$	< 8 ns	yes
optical probe [8]	30 ps	52 mJ cm^{-2} 43 mJ cm^{-2} 33 mJ cm^{-2}	< 5 ns partly back to crystalline partly back to crystalline	yes no no
optical probe [9]	fs scale	59.6 mJ cm^{-2} 53.3 mJ cm^{-2} 36.6 mJ cm^{-2} 10 mJ cm^{-2}	430 ps < 430 ps < 50 ps back to crystalline	yes yes no no
optical probe [23]	fs scale	–	500 fs	no
XANES probe [22]	600 ps	–	< 4 ns	no
theoretical MD [19]	–	19 mJ cm^{-2}	< 24 ps	no

power of the laser, which is proportional to the excitation intensity, can be greatly enhanced with shorter duration. Our simulation [19] represents the limit at which, due to the lack of recombination, all the energy of the short laser pulse can be transferred to electrons before any significant thermalization. However, with increasing duration, recombination eventually completely overlaps with excitation such that effective excitation intensity decreases. For example, Ref. [9] shows that to get amorphization, a fluence of 154 mJ cm^{-2} is needed for $\sim 1 \text{ ns}$ duration, but only 36 mJ cm^{-2} is needed for $\sim 1 \text{ ps}$ duration. As discussed in Ref. [19], the 1-ps duration produces about 15% excitation of the total valence electrons, which is sufficient for a direct collapse of the lattice at room temperature. The excitation intensity for the ns duration is about 1/200 of that for ps duration. Therefore, a 1-ns duration produces only 0.1% excitation, and the effect on lattice destabilization is thus nearly negligible.

6 Conclusions In this review, we address athermal effects in phase transition in PCM materials and, in particular, in GST alloys by ultrafast laser pulse. Microscopic origin for the effect is identified as a quantum-mechanical effect in which the emptying of the Ge–Te antibonding states near the VBM causes lattice instability that drives Ge from sixfold to five, fourfold coordinations. There are a number of ramifications following the understanding: (i) one may utilize the athermal effect to accelerate phase change, at least for the crystalline to amorphous transition; (ii) there exist, indeed, different mechanisms for phase change, more than just the thermal effect. It could well be that the electronic effect discussed here is only a small subset of all possibilities waiting to be uncovered; and (iii) so far, the work has been focused on electronic excitation by optical pulse, not by electrical pulse. One may argue that the latter should not significantly destabilize the host as the amount of electrons removed by an excitation is very limited. However, the effect of the electric field, the role of the material inhomogeneity and beyond may all come into play to alter the picture. Further investigation is expected to offer new strategies to design and manipulate PCM materials for next-generation data storage.

Acknowledgements This work was supported by the NSFC (No. 11104109), the TNList cross-discipline foundation, the China Postdoctoral Science Foundation (No. 2011M500593), and the start-up fund of JLU. SBZ acknowledges the U.S. DOE Office of Basic Energy Sciences (Grant No. DE-SC0002623) and the National Nuclear Security Administration, Office of Nuclear Nonproliferation Research and Engineering (NA-22). We thank

the High Performance Computing Center at JLU for computing resources.

References

- [1] S. R. Ovshinsky, *Phys. Rev. Lett.* **21**, 1450–1453 (1968).
- [2] N. Yamada, E. Ohno, K. Nishiuchi, N. Akahira, and M. Takao, *J. Appl. Phys.* **69**, 2849–2856 (1991).
- [3] M. Wuttig and N. Yamada, *Nature Mater.* **6**, 824–832 (2007).
- [4] A. V. Kolobov, P. Fons, A. I. Frenkel, A. L. Ankudinov, J. Tominaga, and T. Uruga, *Nature Mater.* **3**, 703–708 (2004).
- [5] X. Q. Liu, X. B. Li, L. Zhang, Y. Q. Cheng, Z. G. Yan, M. Xu, X. D. Han, S. B. Zhang, and E. Ma, *Phys. Rev. Lett.* **106**, 025501 (2011).
- [6] D. Lencer, M. Salinga, B. Grabowski, T. Hickel, J. Neugebauer, and M. Wuttig, *Nature Mater.* **7**, 972–977 (2008).
- [7] H.-S. Philip Wong, S. Raoux, S. B. Kim, J. Liang, J. P. Reifenberg, B. Rajendran, M. Asheghi, and K. E. Goodson, *Proc. IEEE* **98**, 2201–2227 (2010).
- [8] J. Siegel, A. Schropp, J. Solis, and C. N. Afonso, *Appl. Phys. Lett.* **84**, 2250–2252 (2004).
- [9] J. Siegel, W. Gawelda, D. Puerto, C. Dorronsoro, J. Solis, C. N. Afonso, J. C. G. de Sande, R. Bez, A. Pirovano, and C. Wiemer, *J. Appl. Phys.* **103**, 023516 (2008).
- [10] S. K. Sundaram and E. Mazur, *Nature Mater.* **1**, 217–224 (2002).
- [11] M. Wautelet, *Phys. Status Solidi B* **138**, 447–456 (1986).
- [12] J. A. Van Vechten, R. Tsu, F. W. Saris, and D. Hoonhout, *Phys. Lett. A* **74**, 417–421 (1979).
- [13] J. A. Van Vechten, R. Tsu, and F. W. Saris, *Phys. Lett. A* **74**, 422–426 (1979).
- [14] E. N. Glezer, Y. Siegal, L. Huang, and E. Mazur, *Phys. Rev. B* **51**, 9589–9596 (1995).
- [15] K. Sokolowski-Tinten, J. Bialkowski, and D. von der Linde, *Phys. Rev. B* **51**, 14186–14198 (1995).
- [16] W. Gawelda, J. Siegel, C. N. Afonso, V. Plausinaitiene, and A. Abrutis, *J. Appl. Phys.* **109**, 123102 (2011).
- [17] A. Schropp, J. Siegel, J. Solis, C. N. Afonso, and M. Wuttig, 2003 Conference on Lasers and Electro-Optics Europe, IEEE Cat. No. 03TH8666, 748 (2003).
- [18] C. Peng and M. Mansuripur, *Appl. Opt.* **43**, 4367–4375 (2004).
- [19] X. B. Li, X. Q. Liu, X. Liu, D. Han, Z. Zhang, X. D. Han, H. B. Sun, and S. B. Zhang, *Phys. Rev. Lett.* **107**, 015501 (2011).
- [20] Y. Miyamoto, H. Zhang, and D. Tomanek, *Phys. Rev. Lett.* **104**, 208302 (2010).
- [21] G. Smolentsev, A. V. Soldatov, and M. C. Feiters, *Phys. Rev. B* **75**, 144106 (2007).
- [22] P. Fons, H. Osawa, A. V. Kolobov, T. Fukaya, M. Suzuki, T. Uruga, N. Kawamura, H. Tanida, and J. Tominaga, *Phys. Rev. B* **82**, 041203(R) (2010).
- [23] H. Santoh, Y. Hongo, K. Tajima, M. Konishi, and T. Saiki, 2009 E/PCOS, available from http://www.epcos.org/epcos2009/Abstracts2009/Abstract_Saiki.pdf 2009.